**FINAL TECHNICAL REPORT**

# Slip rate for the central and southern San Jacinto Fault Zone, southern California: Towards understanding variations in rate over time: Collaborative Proposal between San Diego State University and University of Cincinnati

U.S.G.S GRANT NO. 07HQGR0007
and
U.S.G.S GRANT NO. 07HQGR0017

Thomas Rockwell, P.I.
Geological Sciences
San Diego State University
San Diego, CA 92182
Trockwel@geology.sdsu.edu

and

Lewis Owen, Co-P.I.
Department of Geology
University of Cincinnati
P.O. Box 210013
Cincinnati, OH 45221-0013

Note: This final technical report is written as a paper to be immediately submitted for publication in *Geology*. Hence, the paper title is different from the original proposal title. Kim Le, Caitlin Lippincott and Jason Dortch were involved in this project as part of their graduate training, which include laboratory, fieldwork and the preparation of this paper. Michael Oskin and Marc Caffee were collaborators on this project and contributed to writing the manuscript. In addition, Marc Caffee was responsible for making the $^{10}$Be AMS measurements at PRIME Laboratory.

# Late Quaternary slip rates on the San Jacinto Fault, California: Implications for fault zone initiation and kinematics


| | |
|---|---|
| **Kimberly Le*** | Department of Geological Sciences, University of North Carolina, Chapel Hill, NC 27599, USA |
| **Thomas Rockwell** | Department of Geological Sciences, San Diego State University, San Diego, CA 92182, USA |
| **Lewis A. Owen** | Department of Geology, University of Cincinnati, Cincinnati, OH 45221, USA |
| **Michael Oskin** | Department of Geological Sciences, University of North Carolina, Chapel Hill, NC 27599, USA |
| **Caitlin Lippincott** | Department of Geological Sciences, San Diego State University, San Diego, CA 92181, USA |
| **Marc W. Caffee** | Department of Physics, Purdue University, West Lafayette, IN 47906, USA |
| **Jason Dortch** | Department of Geology, University of Cincinnati, Cincinnati, OH 45221, USA |



## ABSTRACT

The San Andreas and San Jacinto faults are the two principle zones at the southern end of the San Andreas-Gulf of California transform plate boundary, yet their Late Quaternary fault history has not been adequately defined. This information is critical to determine the partitioning of deformation across the plate boundary, the kinematic evolution of the fault zones, and the associated seismic hazard. Geologic field mapping, remote sensing, tectonic geomorphology and $^{10}$Be terrestrial cosmogenic radionuclide dating of faulted landforms were therefore undertaken to provide quantitative Late Quaternary slip rates for the Clark segment of the southcentral and southern stretches of the San Jacinto fault. Beheaded channels in the southcentral stretch date to 54.4 ± 7.5 ka and 32.3 ± 8.5 ka, while faulted alluvial deposits along the southern stretch date to 30.6 ± 6 ka, which yield dextral fault slip rates of 8.4 ± 1.1, and 1.7 ± 0.4 mm/yr, respectively. These slip rates are slower than those for the central and northern stretches of the San Jacinto fault, and imply a slip gradient along the Clark strand from Anza southeastward to its' surface termination. Combining previously published data on Holocene rates of the Coyote Creek fault with measured total bedrock displacement along the southern San



* E-mail: kle@email.unc.edu

Jacinto fault zone suggests that the role of the San Jacinto fault is secondary to the San Andreas fault at the southern end of the plate boundary. Finally, it appears that slip rates for the San Jacinto fault have substantially decreased since fault initiation or that motion began earlier than suggested by some recent studies.

## INTRODUCTION

The San Andreas and the San Jacinto faults are the two main zones at the southern end of the San Andreas-Gulf of California transform plate boundary, and together they account for ~80% of the relative motion between the Pacific and North American plates (Fig. 1; Bennett et al., 2004, Fialko et al., 2006). The San Jacinto fault zone (SJFZ) is historically the most seismically active (Hanks et al., 1975; Thatcher et al., 1975, Richards-Dinger and Shearer, 2000), but its role in accommodating plate boundary motion is controversial. Some researchers suggest that it may be the more dominant fault at the southern end of the plate boundary (Morton and Matti, 1993; Dorsey, 2002; Lutz et al., 2006), whereas others have documented relatively low Holocene slip rates (Clark et al., 1972; Sharp, 1981; Pollard and Rockwell, 1995; Gurrola and Rockwell, 1996; Verdugo et al., 2005). Despite the significance of the SJFZ, its Late Quaternary history and its age of initiation have not been adequately defined. Initiation of the SJF and its evolution as a major right-lateral strike slip fault began as early as 2.4 Ma (Rockwell et al., 1990) to 1.5 Ma (Morton and Matti, 1993) to as recently as ~1.0 Ma (Dorsey, 2002; Lutz et al, 2006, Kirby et al., 2007). Researchers suggest the SJFZ initiated from strain localization along the restraining bend of the San Andreas fault (SAF) and/or prebatholithic structures providing a path of least resistance for slip transfer (Morton and Matti, 1993; Langenhein et al., 2005; Li and Liu, 2007).

Estimates of geologic slip rates across the SJFZ range from as much as 20 mm/yr along the northern segment (Morton and Matti, 1993; Kendrick et al., 2002), to 12-14 mm/yr at Anza (Rockwell 1990) along its central segment, to 3-10 mm/yr along its southern segment (Fig.1)(Sharp 1981; Gurrola and Rockwell, 1996; Pollard and Rockwell, 1995; Dorsey, 2002). Geodetic and interferometric models of strain accumulation across the SJFZ also deduce a variety of slip rates from as low as 8 mm/yr (Bennett et al., 2004), to 15 mm/yr (Fay and Humphreys, 2005), to as high as 21 mm/yr (Fialko, 2006). The ambiguity in the slip rate budget and initiation age for what is quite possibly the main plate boundary structure has significant implications for kinematic fault models in assessing earthquake hazards in southern California, and for understanding the tectonic evolution of transform plate boundaries. In this paper, we present the first Late Quaternary slip rates for the south-central and southern end of the Clark segment of the SJFZ at Rockhouse Canyon and the southern Santa Rosa Mountains (Fig. 1). We compare our new slip rates with previously estimated rates along the northern end of the SJF, and with total bedrock displacement, to make inferences about the long-term slip rate history of the SJF.

## TECTONIC SETTING

The ~230 km long SJFZ extends southeastward from the Big Bend of the SAF at the San Gabriel Mountains with an average strike of ~N45°W, cutting through Cretaceous and Tertiary rocks of the Peninsular Ranges (Fig. 1; Sharp, 1967). Based on the relative continuity and similarity in strike, Sanders and Magistrale (1997) define four

distinct segments for the SJFZ: (1) Claremont, (2) Clark, (3) Coyote Creek, and (4) Superstition segments (Fig. 1B).

Sharp (1967) and Morton and Matti (1993) map the SJFZ cutting through the Peninsular Ranges and found evidence of 20 to 25 km of right lateral displacement. Along the southern SJF, Sharp (1967) estimates the total bedrock displacement at Anza is ~22 km, defined by offset of the Thomas Mountain sill in contact with metamorphic rocks of the Bautista Complex (Fig. 1). Toward Rockhouse Canyon and the southern Santa Rosa Mountains, Cretaceous tonalite and metamorphic rocks, along with Tertiary mylonites, are displaced by ~14.5 km (Fig. 1). Sharp (1967) also documents ~5 km of bedrock displacement for the Coyote Creek segment (Fig.1).

For the Claremont segment, Morton and Matti (1993) and Kendrick et al. (2002) infer a Quaternary slip rate of as much as 20 mm/yr or more, whereas Wesnousky et al. (1991) determined a latest Holocene rate of 1.7-3.3 mm/yr for the main fault strand. To the south along the Coyote Creek segment, Dorsey (2002) suggests a mid-Quaternary to present slip rate of 10 ± 3 mm/yr, whereas Sharp (1981) resolved a mid-Holocene to present slip rate of only 1-2 mm/yr. For the Clark segment at Anza, Rockwell et al. (1990) use soil ages to infer a best-estimated slip rate between 11-13 mm/yr, and Merifield et al. (1991) resolved a mid-Holocene to present rate of 12-17 mm/yr from trenching. Sharp (1981) estimated a minimum mid-Quaternary to present slip rate of 8-12 mm/yr in the same area by reconstructing monolithic alluvial fan deposits to their source. Finally, the 4000-year paleoseismic record at Hog Lake combined with new slip per event data (Middleton, 2006) suggests a mid-late Holocene slip rate of 14-15 mm/yr (Rockwell et al., 2007). These data imply that the Late Quaternary slip rate over multiple

time intervals along the central Clark segment at Anza ranges from 11-17 mm/yr, with best resolved rates between 11-15 mm/yr. Farther south along the Clark segment, there are abundant tectonic landforms that suggest that it is the most active strand in accommodating slip in the southern SJF (Sharp, 1967), especially in comparison to the Coyote Creek segment.

## METHODS

Geomorphic landforms were identified in the field with the aid of Airborne Laser Swath Mapping (ALSM, also known as LiDAR: B4 dataset provided by Southern California Earthquake Center and the US National Science Foundation) along the Clark segment of the SJF. Two detailed study areas were examined, Rockhouse Canyon and a southern Santa Rosa Mountains locality (Fig. 1). A differential GPS was used at these locations, together with the ALSM data, to measure offset landforms and locate exposure age dating sites.

Meter-sized boulders and a 2 m-deep depth profile were sampled for $^{10}$Be terrestrial cosmogenic nuclide exposure dating to define the ages of three different displaced channels and an alluvial surface. Sampling and laboratory methods and age calculations are described in the Appendix 1. Landform exposure ages are affected by geologic factors, which include inheritance of $^{10}$Be by prior exposure, shielding by sediment, toppling and exhumation of boulders, and weathering. Sampling multiple boulders imbricated in debris flow bars within a single channel helps mitigate these problems (Appendix 1). To assess the problem of inherited $^{10}$Be, we sampled the active

channel (Channel 3) at Rockhouse Canyon and a cosmogenic depth profile at the southern Santa Rosa Mountains locality (Figs. 2 and 3).

## ROCKHOUSE CANYON

At Rockhouse Canyon, there are channels in various stages of capture, with two channels (Channel 1 and Channel 2) completely beheaded from their source (Fig. 2). Displacements were determined using channel offsets that were reconstructed based on channel curvature along thefault, with the inference that this form indicates the final stage of channel deflection immediately prior to beheading and capture by another channel (Fig. 2). Displacement for beheaded Channels 1 and 2 are 430 ± 40 m and 150 ± 30 m, respectively. The uncertainties are based on contour curvature of the channel walls on both sides of the fault (Fig. 2). Exposure age samples were collected from these two beheaded channels, along with the active channel, to calculate slip rates. Nine boulders were sampled from each channel to determine the age of the last debris flow event that transported boulders down the channel before beheading. One boulder age from Channel 1 is not used in the calculation of the mean age because the determined $^{10}$Be exposure age yielded an older outlier age (Fig. 3). We collected samples from the active channel, Channel 3, to determine a prior exposure (inheritance of $^{10}$Be) of ~ 7.3 ± 3.0 ka (Fig. 3). The weighted mean age of boulder deposits provides channel abandonment ages of 54.4 ± 7.5 ka for Channel 1 and 32.3 ± 8.5 ka for Channel 2 (Fig. 3 and Appendix 1). Because erosion of the boulder surface will produce younger boulder ages, we re-calculated our ages to represent 2 m/Myr and 5 m/Myr of boulder surface erosion. Incorporting the ages with their displacements yields time-constant slip rates of 8.4 ± 1.1 mm/yr for 0m/Myr of

erosion, 7.5 ± 1.1 mm/yr for 2m/Myr of erosion and 6.1 ± 1.1 mm/yr for 5m/Myr of erosion. This, in turn, requires an interval rate (based on the interval displacement of 280m) between ~54 ka and ~32 ka of as much as 12.9 mm/yr.

## SOUTHERN SANTA ROSA MOUNTAINS

At the Santa Rosa Mountain site, fault displacement was determined using multiple piercing points, including a beheaded channel and two deflected channels (Fig. 2). The alluvial fan surface at this site exhibits strong to moderate desert pavement and varnish development, strong rubification of surface clasts, and a slightly undulating to planar surface morphology. Multiple fault strands vertically displace the surface, but only one shows significant horizontal offset (Fig. 2). Realignment of three channels incised into the alluvial surface define the displacement to 51 ± 5 m (Fig. 2). A cosmogenic depth profile defines the age of the alluvial surface to 30.6 ± 6 ka, yielding a rate of 1.7 ± 0.4 mm/yr (Appendix 1). In turn, we infer that predepositional $^{10}$Be (inheritance) concentrations have been adequately accounted for at both localities, providing confidence in the exposure ages for each site.

## DISCUSSION

Our results suggest spatial slip rate variability along the Clark segment of the SJFZ. At Rockhouse Canyon the time-constant slip rate is 8.4 ± 1.1 mm/yr, however this rate may be lower with increased boulder erosion rates. The ~11-15 mm/yr Late Quaternary slip rate along the Clark segment at Anza (Rockwell et al., 1990) decreases southeastward to 8.4 ± 1.1 mm/yr at Rockhouse Canyon to 1.7 ± 0.4 mm/yr at the

southern Santa Rosa Mountains locality (Fig. 1 and Fig.3). This general southeastward decrease in slip rates along the Clark segment is consistent with a similar decrease in slip per event for the past several events, as documented from small channel offsets (Middleton, 2007). Part of this decrease is likely attributed to folding and thrust faulting (distributed deformation) within the Borrego Badlands and/or a transfer of slip to other faults, such as the Coyote Creek fault (Sharp, 1981; Dorsey 2002; Lutz et al., 2006; Kirby et al., 2006), although there is not a concommitent decrease in bedrock slip. Total bedrock displacement suggests partitioning of slip between the Clark and Coyote Creek segments (Fig. 1), with similar basement offset (14.5 km) at both the Rockhouse Canyon and southern Santa Rosa localities.

The decrease in total bedrock displacement along the Clark segment is consistent with our Late Quaternary slip rate determinations between Anza and Rockhouse Canyon. If we combine the bedrock displacements and slip rates at Anza (22 km and ~13 mm/yr, respectively) and Rockhouse Canyon (14.5 km and ~8.4 mm/yr, respectively), and we assume that this is representative for the life of the fault, the age of fault initiation is ~1.7 Ma. If we take the upper bound of the Rockhouse Canyon rate at 9.5 mm/yr, the Clark segment initiated as late as ~1.5 Ma, similar to the inferred 1.5 Ma fault initiation age of the Claremont segment determined by Morton and Matti (1993) (Fig. 1). Our age of fault initiation is also consistent with geomorphic indicators from relict landscapes along the Clark fault that imply initiation of the SJFZ occurred after 2.0 Ma (Dorsey and Roering, 2005). These findings, however, are at odds with the ~1.1 Ma initiation age interpreted from sedimentary rocks in the Borrego Badlands and the San Felipe Hills (Lutz et al.,

2006, Kirby et al., 2007), which would require a significantly faster rate in the Early Quaternary after initial fault formation.

Taking our Late Quaternary rate (8.4 ± 1.1 mm/yr) as representative of the current strain field, combined with previously published Holocene rates for the Coyote Creek fault (~ 2-5 mm/yr: Clark et al., 1972; Sharp, 1981; Pollard and Rockwell, 1995), suggests that the southern SJFZ accommodates ~10-15 mm/yr of plate boundary motion. This rate is similar to the combined rates of the Superstition Mountain fault (5-9 mm/yr: Gurrola and Rockwell, 1996) and Superstition Hills fault (3-6 mm/yr: Hudnut and Sieh, 1989), which yield an overall rate of ~11-15 mm/yr. This is also consistent with the geodetic strain rates inferred for the southern SJFZ (Bennett, 2004; Fay and Humphreys, 2005), but is slower than the 20 mm/yr suggested by InSAR (Fialko, 2006). Part of the discrepancy may be attributed to distributed deformation by folding and cross-faulting, which is ignored in the InSAR rate. In comparison to the slip rate of the SAF (van der Woerd et al., 2002; Matmon et al., 2005), it appears that the SJF has been slower during the Late Quaternary.

## CONCLUSIONS

Our data document considerable spatial variability, and possible temporal variability, along the southern SAF-Gulf of California transform plate margin during the Quaternary, which suggests complex fault system kinematic evolution. Seismic hazard studies commonly rely on long-term Quaternary rates to infer short term hazard. Our observations suggest that we need information over multiple time frames, along with current (geodetic) and Late Holocene slip rates to adequately address earthquake hazards

along evolving plate margins. Our slower Late Quaternary slip rate estimates of 8.4 ± 1.1 mm/yr at Rockhouse Canyon and 1.7 ± 0.4 mm/yr for the southern Santa Rosa Mountains, if representative for the life of the fault, suggest that 1) the SJF initiated ~1.5-1.7 Ma and 2) it is currently subordinate to the SAF in accommodating plate margin strain. Alternatively, if ths stratigraphic data are correct that the fault initiated closer to 1 Ma, then the SJF has slowed down considerably since its' early history.

**ACKNOWLEDGEMENTS**

This research was supported by NEHRP (07HQGR0007) awarded to T. Rockwell and L.A. Owen and partially supported by the Southern California Earthquake Center (SCEC) awarded to M. Oskin. Special thanks to Alana Wilson and Eitan Shelef for field assistance, George Jefferson and all the Rangers at Anza Borrego State Park for their help throughout the field season. We also thank Dr. Robert Finkel and Dylan Rood AMS for measurements at the Lawrence Livermore National Laboratory.

**REFERENCES CITED**

Bennett, R. A., Friedrich, Anke, M., Furlong, Kevin P (2004). "Codependent histories of the San Andreas and San Jacinto fault zones from inversion of fault displacement rates." Geology 32(11): 961-964.

Dorsey, R. J. (2002). "Stratigraphic record of Pleistocene initiation and slip on the Coyote Creek fault, Lower Coyote Creek, southern California." Geological Society of America Special Paper 365: 251-269.

Fay, N., Humphreys, Eugene D. (2005). "Fault slip rates, effects of elastic heterogeneity on geodetic data, and the strength of the lower crust in the Salton Trough region, southern California." Journal of Geophysical Research 110: 1-14.

Fialko, Y. (2006). "Interseismic strain accummulation and the earthquake potential on the southern San Andreas fault system." Nature 441: 968-971.

Kendrick, K. J., Morton, D.M., Wells, S.G., Simpson, R.W. (2002). "Spatial and Temporal Deformation along the Northern San Jacinto Fault, Southern California:Implications for Slip Rates." Bulletin of the Seismological Society of America 92(7): 2782-2802.

Kirby, S., Janecke, S., Dorsey, R., Housen, B., Langenheim, V., McDougall, K., Steely, A. (2007). "Pleistocene Brawley and Ocotillo Formations: Evidence for Initial Strike-Slip Deformation along the San Felipe and San Jacinto Fault Zones, Southern California." The Journal of Geology 115: 43-62.

Langenheim, V. E., Jachens, R.C., Morton, D.M., Kistler, R.W. Matti, J.C. (2004). "Geophysical and isotopic mapping of preexisting crustal structures that influence the location and development of the San Jacinto fault zone, southern California." Geological Society of America Bulletin 116(9/10): 1143-1157.

Li, Y., Vernon, F.L. (2001). "Characterization of the San Jacinto fault zone near Anza, California, by fault zone trapped waves." Journal of Geophysical Research 106: 30671-30688.

Lutz, A. D., R. Housen, B; Janecke, s (2006). "Stratigraphic record of Pleistocene faulting and basin evolution in the Borrego Badlands, San Jacinto fault, southern California." Geological Society of America Bulletin 118: 1377-1397.

Matmon, A., Schwartz, D.P., Finkel, R., Clemmens, S., Hanks, T (2005). "Dating offset fans along the Mojave section of the San Andreas fault using cosmogenic 26Al and 10Be." Geological Society of America Bulletin 117: 795-807.

Middleton, T.J., 2006, Tectonic geomorphology of the southern Clark fault from Anza southeast to the San Felipe Hills: Implications of slip distribution for recent past earthquakes. Unpublished M.S. thesis, San Diego State University, 109 p.

Morton, D. M., Matti, J.C. (1993). Extension and Contraction within an evolving divergent strike-slip fault complex: The San Andreas and San Jacinto fault zones at their convergence in Southern California. Boulder, Geological Society of America Memoir.

Richards-Dinger, K. S., P (2006). "Earthquake locations in southern California obtained from source specific location terms." JGR-Solid Earth 105: 10939-10960.

Rockwell, T., Loughman, Christopher., Merifield , Paul (1990). "Late Quaternary Rate of Slip Along the San Jacinto fault zone near Anza, Southern California." Journal of Geophysical Research 95(B6): 8593-8605.

Sanders, C. O. (1993). "Interaction of the San Jacinto and San Andreas fault zones, southern California: Triggered earthquake migration and coupled recurrence

intervals." Science 260: 973-975.

Sanders, C. O., Magistrale (1997). "Segmentation of the northern San Jacinto fault zone, southern California." JGR-Solid Earth 102: 27, 453-27.

Sharp, R. V. (1967). "The southern San Jacinto fault, Ca."

Sharp, R. V. (1981). "Variable Rates of Late Quaternary Strike Slip on the San Jacinto Fault Zone, Southern California." Journal of Geophysical Research 86(B3): 1754-1762.

van der Woerd, J., Klinger, Y.,Sieh, K.,Tapponier, P.,Ryerson, F., Meriaux, A (2006). "Long-term slip rate of the southern San Andreas Fault from 10Be-26Al surface exposure dating of an offset alluvial fan." JGR 111.

DR1. SUMMARY OF SAN JACINTO FAULT $^{10}$Be MODEL AGES

| Sample name | Thickness (cm) | Shielding correction | Altitude (m) | Latitude (DD) | Longitude (DD) | $^{10}$Be measured ($10^6$ atom $g^{-1}$) | $^{10}$Be age (ka) 0m/Myr | Error* ± (ka) | $^{10}$Be age (ka) 2m/Myr | Error* ± (ka) | $^{10}$Be age (ka) 5m/Myr | Error* ± (ka) |
|---|---|---|---|---|---|---|---|---|---|---|---|---|
| Channel 1 | | | | | | | | | | | | |
| RH-14 | 1 | 1.000 | 561 | 33.4052 | -116.3708 | 0.4352 ± 0.0155 | 63.7 | 8.4 | 71.5 | 7.7 | 90.2 | 13.0 |
| RH-15 | 3 | 1.000 | 561 | 33.4052 | -116.3707 | 0.4734 ± 0.0163 | 70.6 | 9.2 | 80.3 | 8.8 | 105.4 | 16.3 |
| RH-16 | 4 | 1.000 | 560 | 33.4051 | -116.3707 | 0.3521 ± 0.0363 | 52.7 | 12.7 | 57.9 | 8.7 | 69.1 | 12.8 |
| RH-17† | 2 | 1.000 | 563 | 33.4054 | -116.3708 | 0.5900 ± 0.0346 | 87.5 | 14.6 | 103.2 | 13.3 | 153.9 | 34.5 |
| RH-18 | 2 | 1.000 | 564 | 33.4056 | -116.3709 | 0.4002 ± 0.0137 | 58.9 | 7.6 | 65.5 | 6.9 | 80.4 | 11.0 |
| RH-19 | 4 | 1.000 | 566 | 33.4058 | -116.3709 | 0.3735 ± 0.0268 | 55.7 | 10.4 | 61.6 | 7.8 | 74.5 | 11.9 |
| RH-20 | 2 | 1.000 | 572 | 33.4061 | -116.3710 | 0.2727 ± 0.0406 | 39.7 | 12.9 | 42.6 | 8.0 | 48.0 | 10.3 |
| RH-21 | 5 | 1.000 | 589 | 33.4066 | -116.3712 | 0.3130 ± 0.0143 | 46.2 | 6.7 | 50.1 | 5.4 | 58.0 | 7.4 |
| RH-24 | 5 | 1.000 | 614 | 33.4076 | -116.3710 | 0.3639 ± 0.0106 | 52.8 | 6.4 | 58.0 | 5.9 | 69.1 | 8.7 |
| **Weighted mean of sample ages ± error** | | | | | | | **54.4 ± 7.5** | | **59.4 ± 8.9** | | **69.1 ± 10.4** | |
| Channel 2 | | | | | | | | | | | | |
| RH-33 | 3 | 0.977 | 587 | 33.4061 | -116.3657 | 0.3169 ± 0.0222 | 47.6 | 5.4 | 51.8 | 6.4 | 60.3 | 8.9 |
| RH-34 | 3 | 0.979 | 577 | 33.4053 | -116.3656 | 0.1930 ± 0.0048 | 29.0 | 2.6 | 30.5 | 2.9 | 33.1 | 3.5 |
| RH-35 | 4 | 0.985 | 573 | 33.4046 | -116.3644 | 0.2523 ± 0.0059 | 38.2 | 3.5 | 40.9 | 4.0 | 45.9 | 5.1 |
| RH-36 | 3 | 0.988 | 567 | 33.4039 | -116.3640 | 0.3433 ± 0.0078 | 51.8 | 4.7 | 56.8 | 5.7 | 67.5 | 8.3 |
| RH-37 | 3 | 0.989 | 561 | 33.4033 | -116.3635 | 0.2884 ± 0.0052 | 43.5 | 3.9 | 46.9 | 4.6 | 53.7 | 6.1 |
| RH-38 | 5 | 0.975 | 545 | 33.4025 | -116.3631 | 0.2867 ± 0.0067 | 45.3 | 4.1 | 49.0 | 4.8 | 56.5 | 6.6 |
| RH-39 | 2 | 0.976 | 546 | 33.4017 | -116.3630 | 0.1871 ± 0.0049 | 28.7 | 2.6 | 30.1 | 2.9 | 32.7 | 3.4 |
| RH-40 | 2 | 0.977 | 527 | 33.4039 | -116.3664 | 0.1435 ± 0.0039 | 22.3 | 2.0 | 23.1 | 2.2 | 24.6 | 2.5 |
| **Weighted mean of sample ages ± error** | | | | | | | **32.3 ± 8.5** | | **36.6 ± 9.5** | | **41.1 ± 10.7** | |
| Channel 3 | | | | | | | | | | | | |
| RH-25 | 4 | 1.000 | 587 | 33.4067 | -116.3681 | 0.0333 ± 0.0039 | 4.9 | 1.3 | | | | |
| RH-27 | 3 | 1.000 | 577 | 33.4063 | -116.3680 | 0.0715 ± 0.0044 | 10.5 | 1.8 | | | | |
| RH-28 | 3 | 1.000 | 573 | 33.4060 | -116.3679 | 0.0370 ± 0.0049 | 5.5 | 1.6 | | | | |
| RH-29 | 3 | 1.000 | 567 | 33.4055 | -116.3675 | 0.0893 ± 0.0055 | 13.6 | 2.3 | | | | |
| RH-30 | 4 | 1.000 | 561 | 33.4055 | -116.3675 | 0.0486 ± 0.0038 | 7.5 | 1.5 | | | | |
| RH-31 | 4 | 1.000 | 545 | 33.4046 | -116.3666 | 0.0991 ± 0.0067 | 15.6 | 2.8 | | | | |
| RH-32 | 1 | 1.000 | 546 | 33.4048 | -116.3667 | 0.0397 ± 0.0036 | 6.2 | 1.3 | | | | |
| **Weighted mean of sample ages ± error** | | | | | | | **7.3 ± 3.0** | | | | | |

*Notes:* $^{10}$Be model ages calculated using the CRONUS calculator at Rockhouse Canyon (see Fig. 1 for sample locations).
Abbreviations: DD is decimal degrees,
*External error associated with $^{10}$Be model exposure ages.
†Boulder samples that are not used in the calculation of the weighted mean age. See Appendix for details

Figure 1. Location map showing (A) the major faults for southern California, and (B) the location the study area, and (C) geologic map of the southern San Jacinto fault zone. Red dashed box in part (A) shows the location of the Clark segment. The blue arrows show the amount of displacement of plutonic, metamorphic and mylonitic rocks mapped by Sharp (1967). The white stars indicate the location of localities along the Clark segment discussed in the text.

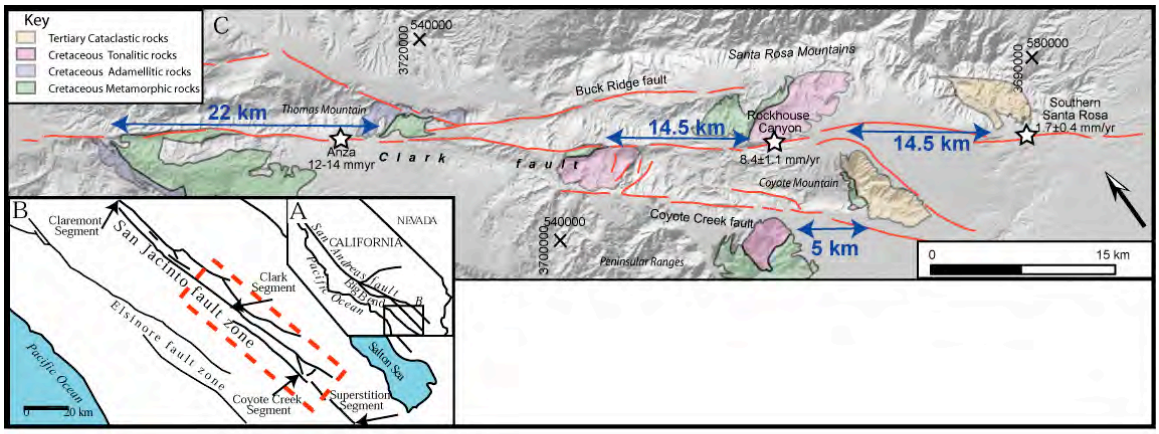

Figure 2. ALSM image of beheaded and deflected channels at Rockhouse Canyon and the southern Santa Rosa Mountains. Rockhouse Canyon (A) reconstruction of Channel 1 immediately before beheading; (B) reconstruction of Channel 2 immediately before beheading; and (C) is the present configuration of Channels 1, 2 and 3. The blue dots in panel C indicate the location of boulder samples collected for $^{10}$Be exposure age dating. See Fig. 1 for location. Santa Rosa Mountains (A) reconstruction of two deflected and one beheaded channel; (B) is the present configuration of channel. The white star is the location of the 2 m deep depth profile sampled for exposure age dating. See text and Appendix 1 for details.

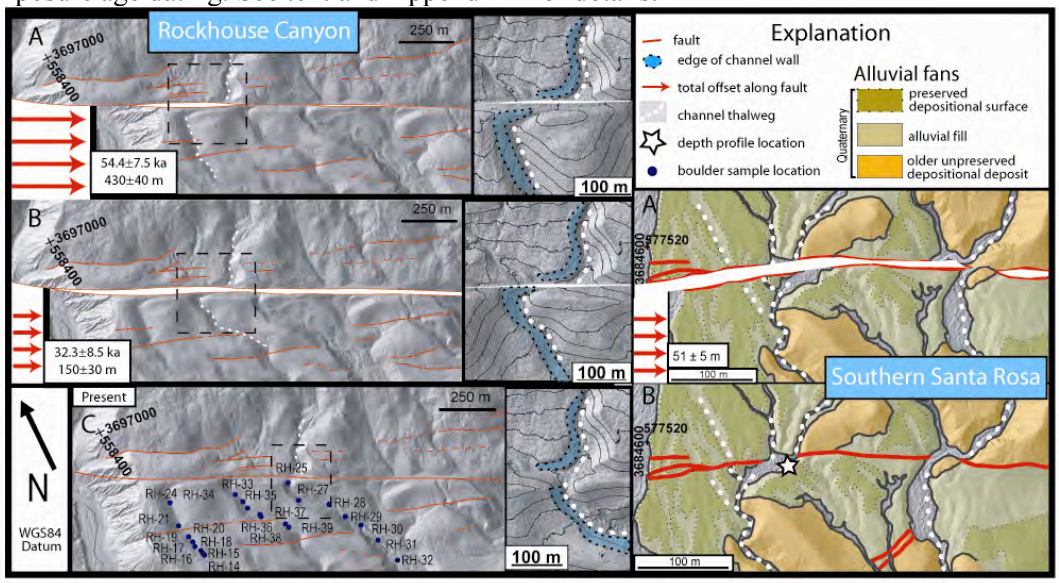

Figure 3. The distribution of ages for the central and southern Clark fault and calculated slip rates. (A) The chart shows the weighted mean age of Channel 1, Channel 2 and Channel 3. Ages reflect inheritance from Channel 3. The red bars are error weighted mean ages used in calculating the age. The blue bar is an outlier that is 2σ outside the error weighted mean age of samples from Channel 1. (B) Exponential decrease in the concentration of $^{10}$Be with depth from an alluvial surface cut by the Clark fault at the southern Santa Rosa Mountain locality. Red lines represent 95% confidence boundary around the regression line. Dotted lines represent the inhertance and its associated errors. The regression line indicates a surface age of 30.8 ± 6 ka. (C) Linear least square fit of ages vs. displacement at Rockhouse Canyon for slip rate determinations. The slip rate shown reflect 0m/Myr, 2m/Myr and 5 m/Myr of erosion of the boulder surface. See text and Appendix 1 for details.

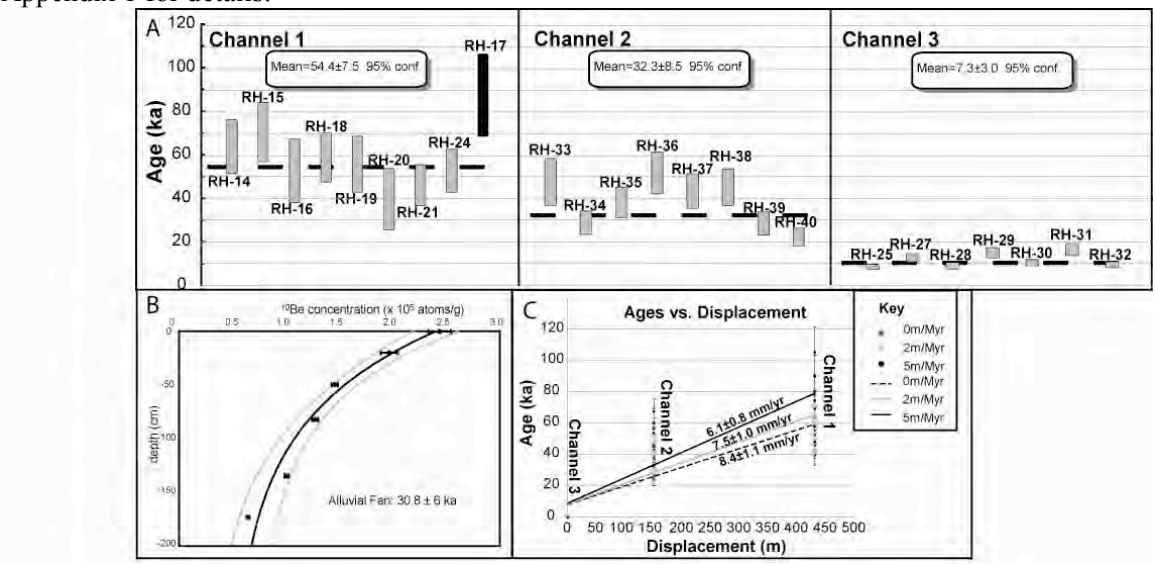

**Appendix 1**

**Sampling methods**

We dated landforms along the Clark fault using $^{10}$Be sampling methods adapted for available material and degradation of the landform. Sample sites were recorded with a handheld GPS unit (Table DR1). At Rockhouse Canyon, samples (~ 600 g) were collected from the tops of granitic boulders lodged within debris flow bars using a hammer and chisle. To determine the age of an offset alluvial fan deposit located along the southern Santa Rosa Mountains, we collected ~2 kg of gravels and pebbles from a 2 m deep cosmogenic depth profile. Six samples were collected from 20 to 40 cm intervals from a natural exposure incised into the alluvial surface. Photographs and notes were recorded at each sampling site to document the degree of weathering and site conditions for each sample.

**Laboratory methods**

Samples were crushed and sieved to obtain the 250 to 500 μm size fraction. This fraction was chemically leached by a minimum of four acid leaches: aqua regia for > 9 hours; two 5% $HF/HNO_3$ leaches for ~ 24 hours; and one or more 1% $HF/HNO_3$ leaches each for ~ 24 hours. To remove acid resistant and mafic minerals, heavy liquid (density of 2.7 g/cm$^3$) separations with lithium heteropolytungstate (LST) were used after the first 5% $HF/HNO_3$ leach. Low background $^9$Be carrier ($^{10}$Be/$^9$Be ~ 1 x $10^{-15}$) was added to pure quartz, which was then dissolved in concentrated HF and fumed with perchloric acid to remove fluoride atoms. Fifteen to thirty grams of quartz was assumed for determining acid volumes used in the processing of chemical blanks. Next, the samples were passed through anion and cation exchange columns to remove Fe and Ti and to separate the $^{10}$Be fraction. Ammonium hydroxide was added to the $^{10}$Be fractions to precipitate beryllium hydroxide gel. The beryllium hydroxide was oxidized by ignition at 750$^o$C for 5 minutes in quartz crucibles. Beryllium oxide was mixed with Nb powder and loaded in steel targets for the measurement of the $^{10}$Be/$^9$Be ratios by accelerator mass spectrometry at CAMS at the Lawrence Livermore National Laboratory or at the PRIME Laboratory at Purdue University.

**Calculations**

All $^{10}$Be ages for boulders samples were calculated using the CRONUS Age Calculator (Balco et al., 2008; http://hess.ess.washington.edu/math/; Table DR1). This uses the scaling factors of Lal (1991) and Stone (2000) and a sea-level low-latitude production rate of 5.1±0.3 $^{10}$Be atoms/gram of quartz/year. No correction was made for geomagnetic field variations due to the ongoing debate regarding which correction factors are most appropriate. The age determined from the depth profile at our Santa Rosa locality is a linear least square line fit that produces uncertainity estimates for fit values of $^{10}$Be concentrations collected from a 2 m depth profile exposed from a natural channel incision (Fig. 3). All ages at Rockhouse Canyon are error weighted mean ages of all samples within the channel that are within 2σ of the weighted average boulder age. Sample RH-17 is an outlier for exposure ages determined for Channel 1 (DR1 and 2; Fig. 3). The slip rate and error associated with the rate is a linear least square fit of the RMS error of both age and offset of the slope of age vs. displacement.